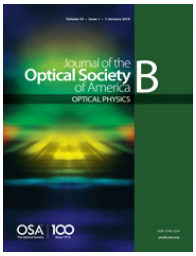

Available online at:
https://www.osapublishing.org/josab/abstract.cfm?uri=josab-30-7-1853

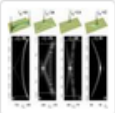

Pulse front distortions caused by primary aberrations
Zoltán L. Horváth, Balázs Major, Attila P. Kovács, and Zsolt Bor
J. Opt. Soc. Am. B **30**(7), 1853-1863 (2013) View: **HTML** | **PDF**

DOI: https://doi.org/10.1364/JOSAB.30.001853

Also selected for

Virtual Journal for Biomedical Optics
Andrew Dunn and Anthony Durkin, Editors

4 September 2013, Volume 8, Issue 8 182 articles

https://www.osapublishing.org/vjbo/virtual_issue.cfm?vid=215

Pulse front distortions caused by primary aberrations

Zoltán L. Horváth, Balázs Major, Attila P. Kovács, and Zsolt Bor
Department of Optics and Quantum Electronics,
University of Szeged, H-6701 Szeged P. O. Box 406, Hungary

A wave optical description of the effect of the primary aberrations on the temporal and spatial shape of an ultrashort pulse is presented. The calculations are based on the diffraction theory of aberrations investigated by Nijboer and Zernike, leading to an effective numerical treatment of Seidel aberrations. The explicit form of the recurrence relations for the coefficients of the circular polynomial expansion are published, as far as we know, for the first time. Comparisons between the results of wave optical and geometrical optical formulas are shown. The appearance of boundary diffraction wave pulse, known from the aberration-free case, is also demonstrated.

PACS numbers: 42.15.Fr, 42.25.Fx

I. INTRODUCTION

Ultrashort laser pulses are widely used in several fields of physics, chemistry and biology, which need the generation of very high intensities in the focal point [1–3]. Focused ultrashort pulses are key elements of experiments related to surface plasmons [4, 5], attosecond physics [6], and particle acceleration [7]; important in the investigation of dynamical processes [8, 9]; and a potential equipment for neurosurgery [10]. All these applications require the knowledge of the spatial and temporal properties of the pulses.

By the rapid progress in the technology of ultrashort pulse lasers, nowadays the pulses are formed by only a few optical cycles [11–13], thus the optical aberrations of the optical elements can alter the spatial and temporal behavior of the pulse, and result in disadvantageous temporal and spatial distortions. The temporal and spatial broadening, or the pulse front distortion, for instance, can decrease the achievable intensity of the focused pulse, or reduce the longitudinal and lateral resolution of a (nonlinear) microscope.

The effect of chromatic aberration on the temporal and spatial shape of an ultrashort pulse has already been studied extensively, both theoretically and experimentally [14–28]. The influence of monochromatic aberrations on the pulse shape, that is the effect of spherical aberration [26–29], astigmatism, coma, curvature of field, and distortion [30, 31] has also been investigated to a certain extent. Direct measurements of the spatio-temporal form of focused pulses distorted by aberrations have also been performed [32–34]. Focused attosecond pulses have been examined similarly as well [35].

The present investigation is concerned with the description of a theoretical treatment of the effect of primary aberrations on the temporal and spatial shape of an ultrashort pulse. Since a short pulse can be represented by the superposition of its monochromatic components, the effect of monochromatic aberrations on the pulse can be calculated by taking into account the effect of aberrations on each spectral component. These effects on a monochromatic component can be treated by the diffraction theory of aberrations investigated by Nijboer and Zernike [36]. Some preliminary results of these calculations have already been presented [37], but this is the first time the details are published.

II. WAVE OPTICAL DESCRIPTION OF THE PULSE PROPAGATION IN THE PRESENCE OF ABERRATIONS

Consider a centered optical system with its axis along CO_1, where C is the center of the exit pupil (see Fig. 1). In the absence of the aberrations the outgoing wave is a

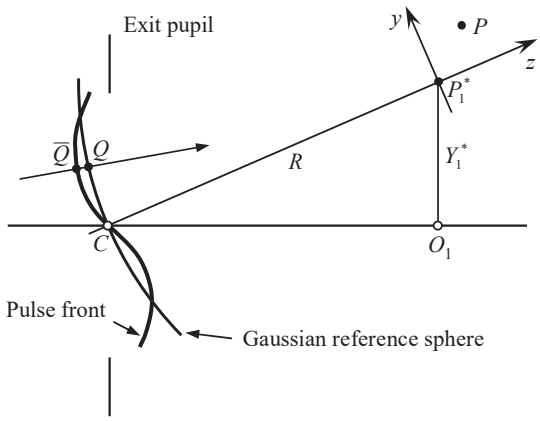

FIG. 1: Interpretation of the aberration function

perfectly spherical wave converging towards the paraxial image point P_1^* . So the disturbance at the Gaussian reference sphere [36] with radius R is given by

$$E_0(Q,t) = \frac{A\,h(t+R/c)}{R}, \tag{1}$$

where Q is the typical point of the Gaussian reference sphere, t is the time, A/R is the amplitude of the disturbance and c is the speed of light. Function

$$h(t) = b(t)\,e^{-i\omega_0 t} \tag{2}$$

describes the arbitrary time evolution of the pulse, where $b(t)$ is the envelope and ω_0 is the carrier angular frequency of the pulse. The origin of the time is chosen so that the pulse front is situated on the Gaussian reference sphere at the time $t = -R/c$, which means that the envelope $b(t)$ has its maximum at $t = 0$.

In the presence of aberrations the wave front differs from the ideal spherical one. The deformation of the wave front is measured by the aberration function Φ, defined as follows [36]. The absolute value $|\Phi|$ represents the distance between the two points $\overline{Q}$ and Q, where $\overline{Q}$ is the point in which a ray passing through the exit pupil intersects the wave front passing through C, and Q is the intersection of the same ray and the Gaussian reference sphere. The value of Φ is taken positive if the direction of $\overrightarrow{\overline{Q}Q}$ coincides with the direction of propagation and Φ is taken negative if $\overrightarrow{\overline{Q}Q}$ has the opposite direction. Since a disturbance emerging at point $\overline{Q}$ reaches point Q over the time interval of $\Delta t = \Phi/c$, the disturbance at the Gaussian reference sphere in the presence of an aberration represented by Φ is given by

$$E(Q,t) = \frac{A\, h(t + (R - \Phi)/c)}{R}. \tag{3}$$

$E(Q,t)$ can be represented in the form of a Fourier integral (i.e. as a composition of monochromatic waves)

$$E(Q,t) = \frac{1}{2\pi} \int_{-\infty}^{\infty} U(Q,\omega)\, e^{-i\omega t}\, d\omega, \tag{4}$$

where $U(Q,\omega)$ are the monochromatic components given by

$$U(Q,\omega) = \int_{-\infty}^{\infty} E(Q,t)\, e^{i\omega t}\, dt\,. \tag{5}$$

Here the symbols $\mathcal{F}$ and $\mathcal{F}^{-1}$ denote the Fourier transformation and its inverse, respectively. By substituting Eq. (3) into Eq. (5) one can obtain

$$U(Q,\omega) = B(\omega - \omega_0)\frac{Ae^{-ik(R-\Phi)}}{R}\,, \tag{6}$$

where $k = \omega/c$ is the wave number and $B(\omega) = \mathcal{F}\{b(t)\}$.

We choose a Cartesian reference system with its origin O at the Gaussian image point P_1^* and with the z-axis along CP_1^* (Fig. 1). Let (r,ψ,z) be the cylindrical polar coordinates of the observation point P, and $(\rho a,\theta,\zeta)$ stands for the cylindrical polar coordinates of point Q, where a is the radius of the exit pupil, $0 \le \rho \le 1$, and the azimuthal angles ψ and θ measured from the y-axis (Fig. 2). Following the treatment described in Ref. 36, the three dimensional distribution of the disturbance of a monochromatic component near the paraxial image point can be calculated by

$$U(P,\omega) = \frac{-i\omega a^2}{2cR^2}\, AB(\omega - \omega_0)\, e^{i\omega z/c}\, Y(u,v,\psi,\Phi)\,, \tag{7}$$

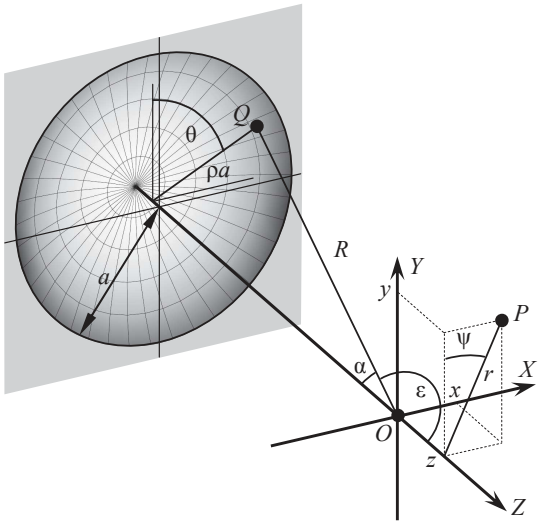

FIG. 2: Choice of the reference frame and notations related to the calculations.

where the function $Y = Y(u,v,\psi,\Phi)$ can be calculated as

$$Y = \frac{1}{\pi}\int_0^1\int_0^{2\pi} e^{i[k\Phi(\rho,\theta) - v\rho\cos(\theta-\psi) - (u/2)\rho^2]}\, d\theta\, \rho\, d\rho\,, \tag{8}$$

in which u and v are the two "optical coordinates" of P given by

$$u = k\,(a/R)^2\, z\,, \tag{9a}$$

$$v = k\,(a/R)\,\sqrt{x^2+y^2} = k\,(a/R)\,r\,, \tag{9b}$$

and (x,y,z) are the Cartesian coordinates of P. The superposition $E(P,t) = \mathcal{F}^{-1}\{U(P,\omega)\}$ of the monochromatic components gives the disturbance

$$E(P,t) = \frac{-ia^2A}{4\pi cR^2}\, e^{-i\omega_0(t-z/c)} \times$$
$$\times \int_{-\infty}^{\infty} (\omega_0 + \Delta\omega)\, B(\Delta\omega) Y\, e^{-i\Delta\omega(t-z/c)}\, d(\Delta\omega)\,, \tag{10}$$

where in the last step Eq. (7) and the substitution of $\Delta\omega = \omega - \omega_0$ have been used. It is worth expressing the coordinates in terms of wavelength associated with the carrier angular frequency ($\lambda_0 = 2\pi c/\omega_0$) and similarly the time in terms of period of the vibration ($T_0 = 2\pi/\omega_0$). Therefore it is convenient to introduce new dimensionless coordinates defined by

$$(\tilde{x},\tilde{y},\tilde{z},\tilde{t}) = \left(\frac{x}{\lambda_0},\frac{y}{\lambda_0},\frac{z}{\lambda_0},\frac{t}{T_0}\right)\,, \tag{11}$$

and to write the pulse envelope in the form of

$$b(t) = \tilde{b}(\gamma\tilde{t}) = \tilde{b}(\gamma t/T_0)\,. \tag{12}$$

After straightforward calculation Eq. (10) can be written in a form of

$$E(P,t) = \frac{-i\pi a^2 A}{\lambda_0 \gamma R^2}\, e^{-i2\pi(\tilde{t}-\tilde{z})} \times \\ \times \int_{-\infty}^{\infty} (1+\Omega)\, \tilde{B}(2\pi\Omega/\gamma)\, Y(u,v,\psi,\Phi)\, e^{-i2\pi\Omega(\tilde{t}-\tilde{z})}\, d\Omega\,, \tag{13}$$

where $\tilde{B}(\omega) = \mathcal{F}\{\tilde{b}(t)\}$, $\Omega = \Delta\omega/\omega_0 = (\omega-\omega_0)/\omega_0$. The variables u, v can also be expressed with the new variables as

$$u = 2\pi(1+\Omega)\,(a/R)^2\,\tilde{z}\,, \tag{14a}$$
$$v = 2\pi(1+\Omega)\,(a/R)\,\tilde{r}\,, \tag{14b}$$

where $\tilde{r} = \sqrt{\tilde{x}^2+\tilde{y}^2} = r/\lambda_0$. If the pulse has Gaussian temporal shape,

$$\tilde{b}(t) = \exp(-t^2)\,, \tag{15a}$$
$$\tilde{B}(\omega) = \sqrt{\pi}\,\exp(-\omega^2/4)\,, \tag{15b}$$
$$\gamma = \sqrt{2\ln 2}\,\frac{T_0}{\tau} = \frac{\sqrt{2\ln 2}}{N}\,, \tag{15c}$$

where τ is the temporal duration of the pulse (FWHM in intensity), and N is the number of optical cycles defined by $\tau = NT_0$.

III. PRIMARY ABERRATIONS

As it is known, each primary aberration represents a wave front distortion of the form [36]

$$\Phi_{lmn}(\rho,\theta) = A_{lmn}\,\rho^n \cos^m\theta\,, \tag{16}$$

where $2l+m+n=4$, $A_{lmn} = a_{lmn}\,(Y_1^*)^{2l+m}$ and a_{lmn} is a constant. For the numerical calculations it is advantageous to write the aberration function as [36]

$$\Phi'_{lmn}(\rho,\theta) = A'_{lmn}\,R_n^m(\rho)\cos m\theta\,, \tag{17}$$

where $R_n^m(\rho)$ are the Zernike radial polynomials. For primary aberrations the relation between the light distributions associated with the two form of the aberration function given by Eq. (16) and Eq. (17) is exposed by the following *displacement theorem* [36]: if Φ and Φ' are two aberration functions such that

$$\Phi' = \Phi + H\rho^2 + K\rho\sin\theta + L\rho\cos\theta + M\,, \tag{18}$$

where H, K, L and M are constants of order of λ, then

$$Y(u,v,\psi,\Phi) = e^{-ikM}\; Y(u',v',\psi',\Phi')\,, \tag{19}$$

where

$$u' = u + 2kH\,, \tag{20a}$$
$$v'\sin\psi' = v\sin\psi + kK\,, \tag{20b}$$
$$v'\cos\psi' = v\cos\psi + kL\,. \tag{20c}$$

If Y is expressed as the function of the variables (x,y,z) instead of (u,v,ψ) Eq. (19) can be written as

$$Y(x,y,z,\Phi) = e^{-ikM}\times \\ \times\, Y(x+(R/a)K, y+(R/a)L, z+(R/a)^2H, \Phi'). \tag{21}$$

Following the treatment described in Ref. 36 it can be shown that

$$Y(u,v,\psi,\Phi'_{lmn}) = \sum_{p=0}^{\infty} C_p\,(i\alpha_{lnm})^p \times \\ \times \sum_{\substack{0\le q\le p \\ q\equiv p \pmod 2}} (-i)^{qm}\, D_{pq}\, I_{pq}^{(n,m)}(u,v)\,\cos(qm\psi)\,, \tag{22}$$

where $C_p = 2^{2-p}/p\,!$, $\alpha_{lnm} = kA'_{lnm}$,

$$D_{pq} = \binom{p}{(p-q)/2}', \tag{23}$$

$$I_{pq}^{(n,m)}(u,v) = \int_0^1 e^{-i(u/2)\rho^2}\,[R_n^m(\rho)]^p\, J_{qm}(\rho v)\,\rho\, d\rho\,, \tag{24}$$

and $J_n(x)$ are the Bessel functions of the first kind. Here the prime on the binomial coefficient in Eq. (23) indicates that the terms with $q=0$ are to be taken with a factor $1/2$. In Eq. (22) $q \equiv p \pmod 2$ means that q and p are congruent modulo 2, that is q is a even number if p is even, and q is an odd number if p is odd. Using the method described in Ref. 36 one can show that

$$I_{pq}^{(n,m)}(u,v) = e^{-i\,u/4}\sum_{s=0}^{\infty}(-i)^s\,(2s+1)\,j_s(u/4)\times \\ \times \sum_{\substack{j\in N_p \\ w_{sj}^{(p)}\ge mq}} (-1)^{(w_{sj}^{(p)}-mq)/2}\, A_j^{(p,q)}\,\frac{J_{w_{sj}^{(p)}+1}(v)}{v}\,, \tag{25}$$

where $j_s(x)$ are the spherical Bessel functions of the first kind, $A_j^{(p,q)}$ are the coefficients of the finite linear combination of Zernike polynomials (with a prescribed upper index mq) representing of product of two Zernike polynomials:

$$[R_n^m(\rho)]^p\, R_{2s}^0(\rho) = \sum_{\substack{j\in N_p \\ w_{sj}^{(p)}\ge mq}} A_j^{(p,q)}\, R_{w_{sj}^{(p)}}^{mq}(\rho)\,. \tag{26}$$

Here $N_p = N_p(n,m)$ is a finite set of integers and $w_{sj}^{(p)}$ denote the lower indexes of the Zernike polynomials. The coefficients $A_j^{(p,q)}$ depend on the values of s, n and m, and similarly the lower indexes $w_{sj}^{(p)}$ also depend on n and m, but the explicit form of these dependencies are omitted here to simplify the notations. The values of $A_j^{(p,q)}$ and

$w_{sj}^{(p)}$, and the set N_p will be described below for the primary aberrations. These relations can be calculated from the explicit form of $R_n^m(\rho)$ and the recurrence relations of the Zernike polynomials given by [38]

$$2\rho\, R_n^m(\rho) = \frac{n-m}{n+1}\, R_{n-1}^{m+1}(\rho) + \frac{n+m+2}{n+1}\, R_{n+1}^{m+1}(\rho)\ , \tag{27a}$$

$$\begin{aligned} 4(n+1)\rho^2 R_n^m(\rho) &= \frac{n^2-m^2}{n}\, R_{n-2}^m(\rho) \\ &+ \left[\frac{(n+m)^2}{n} + \frac{(n-m+2)^2}{n+2}\right] R_n^m(\rho) \\ &+ \frac{(n+2)^2-m^2}{n+2}\, R_{n+2}^m(\rho)\ . \end{aligned} \tag{27b}$$

A. Primary spherical aberration

As it is known [36], in this case $n=4$ and $l=m=0$, and so $qm=0$. Hence $I_{pq}^{(4,0)}$ (see Eq. (24)) and consequently $A_j^{(p,q)}$ do not depend on q. Therefore q is omitted from their notations, that is they will be denoted by $I_p^{(4,0)}$ and $A_j^{(p)}$, respectively. Using the explicit form $R_4^0(\rho) = 6\rho^4 - 6\rho^2 + 1$ and the recurrence relations of the Zernike polynomials one can show that $N_p = \{0,1,2,\ldots,2p\}$, $w_{sj}^{(p)} = 2[s-2(p-j)]$, and Eq. (25) has a form of

$$\begin{aligned} I_p^{(4,0)}(u,v) &= e^{-i\,u/4}\sum_{s=0}^{\infty}(i)^s\,(2s+1)\,j_s(u/4)\times \\ &\times \sum_{\substack{j=0 \\ s-2(p-j)\ge 0}}^{2p} A_j^{(p)}(s)\,\frac{J_{2[s-2(p-j)]+1}(v)}{v}\ , \end{aligned} \tag{28}$$

with the $A_j^{(p)}$ coefficients of indexes $p=0,1$ given by

$$A_0^{(0)}(s) = 1\ , \tag{29a}$$

$$A^{(1)}(s) = \frac{3}{16}\begin{bmatrix} 2-\frac{1}{2s-1}-\frac{3}{2s+1} \\ \frac{4}{3}+\frac{1}{2s-1}-\frac{1}{2s+3} \\ 2+\frac{3}{2s+1}+\frac{1}{2s+3} \end{bmatrix}\ , \tag{29b}$$

where the values of $A_j^{(1)}$ are arranged as the elements of a column vector for $j=0,1,2$ from top to bottom, respectively. Furthermore, for $p\ge 2$ the coefficients $A_j^{(p)}(s)$ can be calculated by the recurrence relation

$$A_k^{(p)}(s) = \sum_{l=0}^{2} A_{k-l}^{(p-1)}(s)\; A_l^{(1)}[s-2(p-1)+2(k-l)], \tag{30}$$

($k\in N_p = \{0,1,2,\ldots,2p\}$) if we require that $A_j^{(p)}(s) = 0$ when $j\notin N_p$. Using the properties of the binomial coefficients one can obtain

$$Y(u,v,\psi,\Phi'_{040}) = \sum_{p=0}^{\infty}\frac{(i\alpha_{040})^p}{p\,!}\, I_p^{(4,0)}(u,v), \tag{31}$$

where $\alpha_{040} = kA'_{040}$. If the aberration function is represented by the Seidel term Φ_{040} (see Eq. (16)), one can apply the displacement theorem which results in

$$Y(u,v,\psi,\Phi_{040}) = e^{-ikA_{040}/6}\, Y(u-2kA_{040},v,\psi,\Phi'_{040})\ , \tag{32}$$

where $A'_{040} = A_{040}/6$ in Eq. (17).

B. Primary coma

As it is known [36], this case is characterized by $l=0$, $n=3$ and $m=1$. Using the explicit form $R_3^1(\rho) = 3\rho^3 - 2\rho$ and the recurrence relations of the Zernike polynomials one can show that $N_p = \{0,1,2,\ldots,3p\}$ and $w_{sj}^{(p)} = 2s-3p+2j$, so Eq. (25) can be written as

$$\begin{aligned} I_{pq}^{(3,1)}(u,v) &= e^{-i\,u/4}(-1)^{(p-q)/2}\sum_{s=0}^{\infty}(i)^s\,(2s+1)\,j_s(u/4)\times \\ &\times \sum_{\substack{j=0 \\ 2s-3p+2j\ge q}}^{3p}(-1)^j\, A_j^{(p,q)}(2s)\,\frac{J_{2s-3p+2j+1}(v)}{v}\ , \end{aligned} \tag{33}$$

with $A_j^{(p,q)}$ coefficients of indexes $p=0,1,2$ given by

$$A_0^{(0,0)}(s) = 1\ , \tag{34a}$$

$$A^{(1,1)}(s) = \frac{1}{16}\begin{bmatrix} 6-\frac{3}{s-1}+\frac{9}{s+1} \\ 2+\frac{3}{s-1}+\frac{1}{s+1} \\ 2-\frac{1}{s+1}-\frac{3}{s+3} \\ 6+\frac{9}{s+1}+\frac{3}{s+3} \end{bmatrix}\ , \tag{34b}$$

$$A^{(2,0)}(s) = \frac{1}{64}\begin{bmatrix} 9-\frac{27}{8(s-3)}-\frac{27}{4(s-1)}-\frac{135}{8(s+1)} \\ 6-\frac{3}{s-1}-\frac{9}{s+1} \\ 7+\frac{27}{8(s-3)}-\frac{29}{8(s+1)}-\frac{27}{4(s+3)} \\ 20+\frac{3}{s-1}-\frac{3}{s+3} \\ 7+\frac{27}{4(s-1)}+\frac{29}{8(s+1)}-\frac{27}{8(s+5)} \\ 6+\frac{9}{s+1}+\frac{3}{s+3} \\ 9+\frac{135}{8(s+1)}+\frac{27}{4(s+3)}+\frac{27}{8(s+5)} \end{bmatrix}\ , \tag{34c}$$

$$A^{(2,2)}(s) = \frac{1}{64}\begin{bmatrix} 9-\frac{81}{8(s-3)}-\frac{45}{4(s-1)}-\frac{189}{8(s+1)} \\ 6+\frac{9}{s-1}+\frac{3}{s+1} \\ 7+\frac{81}{8(s-3)}-\frac{255}{8(s+1)}-\frac{45}{4(s+3)} \\ 20-\frac{9}{s-1}+\frac{9}{s+3} \\ 7+\frac{45}{4(s-1)}+\frac{255}{8(s+1)}-\frac{81}{8(s+5)} \\ 6-\frac{3}{s+1}-\frac{9}{s+3} \\ 9+\frac{189}{8(s+1)}+\frac{45}{4(s+3)}+\frac{81}{8(s+5)} \end{bmatrix}\ , \tag{34d}$$

where the values of $A_j^{(p,q)}$ are arranged as the elements of a column vector for increasing values of j from top to bottom. If we presume (as before) that $A_j^{(p,q)}(s) = 0$ when $j\notin N_p$, the coefficients $A_j^{(p,q)}(s)$ ($p\ge 2$) are given by recurrence relations

$$A_k^{(p,0)}(s) = \sum_{l=0}^{6} A_{k-l}^{(p-2,0)}(s)\; A_l^{(2,0)}(s-3(p-2)+2(k-l)) \quad \text{if} \;\; q=0\;, \tag{35a}$$

$$A_k^{(p,q)}(s) = \sum_{l=0}^{3} A_{k-l}^{(p-1,q-1)}(s)\; G_l(s-3(p-1)+2(k-l), q-1) \quad \text{if} \;\; q\neq 0\;, \tag{35b}$$

$$G(n,m) = \frac{3}{8}\begin{bmatrix} 1+\frac{(m-1)(m+1)^2}{2(n-1)} - \frac{m^2(m+2)}{n} + \frac{(m-1)(m+1)(m+3)}{2(n+1)} \\ \frac{1}{3} - \frac{(m-1)(m+1)^2}{2(n-1)} + \frac{(3m+1)^2(m+1)}{6(n+1)} - \frac{m^2(m+2)}{n+2} \\ \frac{1}{3} + \frac{m^2(m+2)}{n} - \frac{(3m+1)^2(m+1)}{6(n+1)} - \frac{(m-1)(m+1)^2}{2(n+3)} \\ 1 - \frac{(m-1)(m+1)(m+3)}{2(n+1)} + \frac{m^2(m+2)}{n+2} - \frac{(m-1)(m+1)^2}{2(n+3)} \end{bmatrix} \tag{36}$$

where $k \in N_p = \{0,1,2,\ldots,3p\}$, and the values of $G_l(n,m)$ with increasing l are arranged as the elements of vector (36). In this case Eq. (22) has the form of

$$Y(u,v,\psi,\Phi'_{031}) = \sum_{p=0}^{\infty} C_p\,(i\alpha_{031})^p \times \\ \times \sum_{\substack{0\le q\le p \\ q\equiv p \pmod 2}} (-i)^q\, D_{pq}\, I_{pq}^{(3,1)}(u,v)\,\cos(q\psi)\;, \tag{37}$$

where $\alpha_{031} = kA'_{031}$. If the aberration function is represented by the Seidel term Φ_{031} (see Eq. (16)), one can apply the displacement theorem, which yields

$$Y(x,y,z,\Phi_{031}) = Y(x, y-2(R/a)A_{031}/3, z, \Phi'_{031})\;, \tag{38}$$

where $A'_{031} = A_{031}/3$ in Eq. (17).

C. Primary astigmatism

As it is known [36], we now have $l=0$, $n=m=2$. Using the explicit form $R_2^2(\rho)=\rho^2$ and the recurrence relations of the Zernike polynomials one can show that $N_p = \{0,1,2,\ldots,2p\}$, $w_{sj}^{(p)} = 2(s-p+j)$, and Eq. (25) becomes

$$I_{pq}^{(2,2)}(u,v) = e^{-i\,u/4}\sum_{s=0}^{\infty}(i)^s\,(2s+1)\,j_s(u/4)\times \\ \times \sum_{\substack{j=0 \\ s-p+j\ge q}}^{2p} (-1)^j\, A_j^{(p,q)}(2s)\,\frac{J_{2(s-p+j)+1}(v)}{v}\;, \tag{39}$$

with $A_j^{(p,q)}$ coefficients of indexes $p=0,1,2$ given by

$$A_0^{(0,0)}(s) = 1\;, \tag{40a}$$

$$A^{(1,1)}(s) = \frac{1}{4}\begin{bmatrix} 1-\frac{3}{s+1} \\ 2 \\ 1+\frac{3}{s+1} \end{bmatrix}\;, \tag{40b}$$

$$A^{(2,0)}(s) = \frac{1}{32}\begin{bmatrix} 2-\frac{1}{s-1}-\frac{3}{s+1} \\ 8-\frac{8}{s+1} \\ 12+\frac{1}{s-1}-\frac{1}{s+3} \\ 8+\frac{8}{s+1} \\ 2+\frac{3}{s+1}+\frac{1}{s+3} \end{bmatrix}\;, \tag{40c}$$

$$A^{(2,2)}(s) = \frac{1}{32}\begin{bmatrix} 2-\frac{15}{s-1}-\frac{35}{s+1} \\ 8-\frac{40}{s+1} \\ 12+\frac{15}{s-1}-\frac{15}{s+3} \\ 8+\frac{40}{s+1} \\ 2+\frac{35}{s+1}+\frac{15}{s+3} \end{bmatrix}\;, \tag{40d}$$

where the values of $A_j^{(p,q)}$ are arranged as the elements of a column vector for increasing values of j. If we suppose that $A_j^{(p,q)}(s) = 0$ when $j \notin N_p$, the coefficients $A_j^{(p,q)}(s)$ $(p \ge 2)$ can be calculated by the recurrence relation

$$A_k^{(p,0)}(s) = \sum_{l=0}^{4} A_{k-l}^{(p-2,0)}(s)\ A_l^{(2,0)}(s-2(p-2)+2(k-l)) \quad \text{if} \quad q=0\ , \tag{41a}$$

$$A_k^{(p,q)}(s) = \sum_{l=0}^{2} A_{k-l}^{(p-1,q-1)}(s)\ D_l(s-2(p-1)+2(k-l),2(q-1)) \quad \text{if} \quad q\neq 0\ , \tag{41b}$$

where $k \in N_p = \{0,1,2,\ldots,2p\}$, and by arranging the values of $D_l(n,m)$ with increasing l as the elements of a vector

$$D(n,m) = \frac{1}{4}\begin{bmatrix} 1+\frac{m(m+2)}{n}-\frac{(m+1)(m+3)}{n+1} \\ 2-\frac{m(m+2)}{n}+\frac{m(m+2)}{n+2} \\ 1+\frac{(m+1)(m+3)}{n+1}-\frac{m(m+2)}{n+2} \end{bmatrix}\ . \tag{42}$$

In this case Eq. (22) has the form of

$$Y(u,v,\psi,\Phi'_{022}) = \sum_{p=0}^{\infty} C_p\,(i\alpha_{022})^p \times \\ \times \sum_{\substack{0\le q\le p \\ q\equiv p \pmod 2}} (-1)^q\, D_{pq}\, I_{pq}^{(2,2)}(u,v)\,\cos(2q\psi)\ , \tag{43}$$

where $\alpha_{022} = kA'_{022}$. If the aberration function is represented by the Seidel term Φ_{022} (see Eq. (16)), one can apply the displacement theorem, which yields

$$Y(u,v,\psi,\Phi_{022}) = Y(u-kA_{022},v,\psi,\Phi'_{022})\ , \tag{44}$$

where $A'_{022} = A_{022}/2$ in Eq. (17).

D. Primary curvature of field

This case is represented by $l=1$, $n=2$ and $m=0$. Using the displacement theorem one can obtain

$$Y(u,v,\psi,\Phi_{120}) = Y(u-2kA_{120},v,\psi,\Phi=0)\ . \tag{45}$$

In the absence of chromatic aberration A_{120} does not depend on the frequency, so the integration in Eq. (13) can be carried out. Substituting Eq. (45) into Eq. (13) one can obtain.

$$E(x,y,z,t) = E_0(x,y,z-\Delta z_{120},t-\Delta z_{120}/c)\ , \tag{46}$$

where $E_0(x,y,z,t)$ is the disturbance in the absence of aberrations (i.e. $E(P,t)$ in case of $\Phi=0$), and

$$\Delta z_{120} = 2(R/a)^2\, A_{120}\ . \tag{47}$$

This shows that the effect of this aberration is equivalent to the spatial and temporal shift of the intensity distribution of the aberration free intensity distribution, in contrast to the monochromatic waves, which can be treated by only the spatial shift of the aberration free intensity distribution [36].

E. Primary distortion

For this case $l=1$, $n=1$ and $m=1$. Using again the displacement theorem one can get

$$Y(x,y,z,\Phi_{111}) = Y(x,y-(R/a)A_{111},z,\Phi=0)\ . \tag{48}$$

In the absence of chromatic aberration A_{120} does not depend on the frequency, thus Eq. (48) and Eq. (13) yield

$$E(x,y,z,t) = E_0(x,y-\Delta y_{111},z,t)\ , \tag{49}$$

where

$$\Delta y_{111} = (R/a)\, A_{111}\ . \tag{50}$$

This means that the effect of this aberration is equivalent to the spatial shift of the intensity distribution of the aberration free intensity distribution, similarly to the monochromatic waves [36].

IV. GEOMETRICAL OPTICAL DESCRIPTION OF THE DISTORTION OF THE PULSE FRONT

Since the aberration function Φ measures the deformation of pulse front compared to the Gaussian reference sphere, the distance $O\overline{Q}$ can be approximated by $\overline{R} = R+\Phi$. Using the notation of Fig. 2, the pulse front at the time $t=-R/c$ coincides with a surface defined by

$$S(\overline{R},\alpha,\theta) = R\ , \tag{51}$$

where

$$S(\overline{R},\alpha,\theta) = \overline{R} - \Phi(\alpha,\theta), \tag{52}$$

and Φ is written as the function of variables (α,θ) instead of (ρ,θ). Since the light rays are orthogonal to the wave front, and the light propagates with a velocity of c along a ray, the pulse front at the time t is given by

$$\vec{r}(t,\alpha,\theta) = \vec{r}_{\overline{Q}} + c\,(t-R/c)\,\vec{q}/|\vec{q}|\ , \tag{53}$$

where

$$\vec{r}_{\overline{Q}}(\alpha,\theta) = [R+\Phi(\alpha,\theta)]\times \\ \times(\sin\theta\sin\alpha\,\vec{e}_x + \cos\theta\sin\alpha\,\vec{e}_y - \cos\alpha\,\vec{e}_z) \tag{54}$$

is the position vector of $\overline{Q}$, and

$$\vec{q} = -\mathrm{grad}\, S \tag{55}$$
$$= \left(-\sin\theta\,\sin\alpha + \frac{\sin\theta\,\cos\alpha}{R+\Phi}\,\frac{\partial\Phi}{\partial\alpha}\right. \tag{56}$$
$$\left. + \frac{\cos\theta}{(R+\Phi)\sin\alpha}\frac{\partial\Phi}{\partial\theta}\right)\vec{e}_x \tag{57}$$
$$+\left(-\cos\theta\,\sin\alpha + \frac{\cos\theta\,\cos\alpha}{R+\Phi}\,\frac{\partial\Phi}{\partial\alpha}\right. \tag{58}$$
$$\left. - \frac{\sin\theta}{(R+\Phi)\sin\alpha}\frac{\partial\Phi}{\partial\theta}\right)\vec{e}_y + \tag{59}$$
$$+\left(\cos\alpha + \frac{\sin\alpha}{R+\Phi}\,\frac{\partial\Phi}{\partial\alpha}\right)\vec{e}_z \tag{60}$$

is the direction of the ray at $\overline{Q}$, and the Cartesian unit vectors are denoted by $\vec{e}_x$, $\vec{e}_y$, $\vec{e}_z$. If $t_0 = t_0(\alpha,\theta)$ is the time for which

$$c\,t_0 = |\vec{q}|\Phi + (|\vec{q}|-1)R\ , \tag{61}$$

Eq. (53) can be written in a form of

$$\vec{r}(t,\alpha,\theta) = \vec{r}_0 + c\,(t-t_0)\,\vec{q}/|\vec{q}|\ , \tag{62}$$

where

$$\vec{r}_0 = \left(\sin\theta\,\cos\alpha\frac{\partial\Phi}{\partial\alpha} + \frac{\cos\theta}{\sin\alpha}\frac{\partial\Phi}{\partial\theta}\right)\vec{e}_x$$
$$+\left(\cos\theta\,\cos\alpha\,\frac{\partial\Phi}{\partial\alpha} - \frac{\sin\theta}{\sin\alpha}\frac{\partial\Phi}{\partial\theta}\right)\vec{e}_y \tag{63}$$
$$+\sin\alpha\,\frac{\partial\Phi}{\partial\alpha}\,\vec{e}_z\ .$$

A. Primary aberrations

Since $\rho a/R = \sin\alpha$, the aberration function defined by Eq. (16) can be written in a form of

$$\Phi_{lnm}(\alpha,\theta) = K_{lnm}\,\sin^n\alpha\,\cos^m\theta\ , \tag{64}$$

where $K_{lnm} = A_{lnm}(R/a)^n$.

1. Spherical aberration

In case of primary spherical aberration $l=0$, $n=4$ and $m=0$, so we have now $\Phi = \Phi_{040} = K_{040}\sin^4\alpha$, where $K_{040} = A_{040}(R/a)^4$. Because of the cylindrical symmetry respect to the z-axis, it is enough to calculate the pulse front in a plane containing the axis. We will describe the pulse front in the meridional plane determined by $\theta = 0$. Substituting $\Phi = \Phi_{040} = K_{040}\sin^4\alpha$ into Eq. (55), Eq. (61) and Eq. (63) and supposing $\theta = 0$ one can obtain

$$\vec{q} = \left(1+\frac{4\Phi}{R+\Phi}\right)\times$$
$$\times\left[\cos\alpha\,\vec{e}_z - \sin\alpha\left(1-\frac{4K\sin^2\alpha}{R+5\Phi}\right)\vec{e}_y\right], \tag{65a}$$
$$\vec{r}_0 = 4\Phi\cos\alpha\,\vec{e}_z - 4(\Phi - K\sin\alpha)\sin\alpha\,\vec{e}_y\ , \tag{65b}$$
$$c\,t_0 = |\vec{q}|\Phi + (|\vec{q}|-1)R =$$
$$= \Phi\left(1 - 8\frac{\Phi - K\sin^2\alpha}{R} - 8\frac{\Phi}{R}\frac{K\sin^2\alpha}{R} - \dots\right)\ , \tag{65c}$$

where the notations $\Phi = \Phi_{040}$ and $K = K_{040}$ are used for the sake of the brevity, and in the last step ct_0 is expanded in power series. For practical cases $|\Phi| \ll R$ and thus $|K| \ll R$, then $\vec{q} \approx \cos\alpha\,\vec{e}_z - \sin\alpha\,\vec{e}_y$ (so $|\vec{q}| \approx 1$) and $c\,t_0 \approx \Phi$. The pulse front in the meridional plane is determined by Eq. (62) with Eq. (65).

2. Coma

In this case $l=0$, $n=3$ and $m=1$, so $\Phi = \Phi_{031} = K_{031}\sin^3\alpha\,\cos\theta$, where $K_{031} = A_{031}(R/a)^3$. Substituting $\Phi = \Phi_{031}$ into Eq. (55), Eq. (61) and Eq. (63) one can obtain

$$\vec{q} = \left(1+\frac{3\Phi}{R+\Phi}\right)\left\{-\sin\theta\,\sin\alpha\left(1-\frac{2K\sin\alpha\,\cos\theta}{R+4\Phi}\right)\vec{e}_x + \right.$$
$$\left. + \left[-\cos\theta\,\sin\alpha\left(1-\frac{2K\sin\alpha\,\cos\theta}{R+4\Phi}\right) + \frac{K\sin^2\alpha}{R+4\Phi}\right]\vec{e}_y + \cos\alpha\,\vec{e}_z\right\}\ , \tag{66a}$$
$$\vec{r}_0 = 3\Phi\cos\alpha\,\vec{e}_z + (2K\sin\alpha\,\cos\theta - 3\Phi)\sin\alpha\,\sin\theta\,\vec{e}_x +$$
$$+ \left[(2K\sin\alpha\,\cos\theta - 3\Phi)\sin\alpha\,\cos\theta + K\sin^2\alpha\right]\vec{e}_y\ , \tag{66b}$$
$$c\,t_0 = |\vec{q}|\Phi + (|\vec{q}|-1)R =$$
$$= \Phi + \frac{K^2\sin^4\alpha + 2\Phi K\sin\alpha\cos\theta - 9\Phi^2}{2R} + \frac{9\Phi^3 - 8\Phi^2 K\sin\alpha\cos\theta - \Phi K^2\sin^4\alpha}{2R^2} + \dots\ , \tag{66c}$$

where the notations $\Phi = \Phi_{031}$ and $K = K_{031}$ are used for the sake of the brevity, and in the last step ct_0 is expanded in power series. For practical cases $|\Phi| \ll R$ and thus $|K| \ll R$, then $\vec{q} \approx \cos\alpha\,\vec{e}_z - \sin\theta\,\sin\alpha\,\vec{e}_x - \cos\theta\,\sin\alpha\,\vec{e}_y$ (so $|\vec{q}| \approx 1$) and $c\,t_0 \approx \Phi$. The pulse front is determined by Eq. (62) with Eq. (66).

3. Astigmatism

In case of primary astigmatism $l = 0$, $n = 2 = m = 2$, thus $\Phi = \Phi_{022} = K_{022}\sin^2\alpha\,\cos^2\theta$, where $K_{022} = A_{022}(R/a)^2$. Substituting $\Phi = \Phi_{022}$ into Eq. (55), Eq. (61) and Eq. (63) one can obtain

$$\vec{q} = \left(1 + \frac{2\Phi}{R+\Phi}\right) \times \times \left\{ -\sin\theta\,\sin\alpha\,\vec{e}_x - \cos\theta\,\sin\alpha\left(1 - \frac{2K}{R+3\Phi}\right)\vec{e}_y + \cos\alpha\,\vec{e}_z \right\}\ , \tag{67a}$$

$$\vec{r}_0 = 2\Phi\cos\alpha\,\vec{e}_z - 2\Phi\sin\alpha\,\sin\theta\,\vec{e}_x + 2(K-\Phi)\sin\alpha\,\cos\theta\,\vec{e}_y \tag{67b}$$

$$c\,t_0 = |\vec{q}|\Phi + (|\vec{q}|-1)R = = \Phi\left(1 - 2\frac{\Phi - K}{R} - 2\frac{\Phi}{R}\frac{K}{R} - \dots\right)\ , \tag{67c}$$

where the notations $\Phi = \Phi_{022}$ and $K = K_{022}$ are used for the sake of the brevity, and in the last step ct_0 is expanded in power series. For practical cases $|\Phi| \ll R$ and thus $|K| \ll R$, then $\vec{q} \approx \cos\alpha\,\vec{e}_z - \sin\theta\,\sin\alpha\,\vec{e}_x - \cos\theta\,\sin\alpha\,\vec{e}_y$ (so $|\vec{q}| \approx 1$) and $c\,t_0 \approx \Phi$. The pulse front is determined by Eq. (62) with Eq. (67).

V. RESULTS AND DISCUSSION

The intensity given by $I = |E|^2$ was calculated from Eq. (13) assuming $a/R = 0.1$ and Gaussian temporal envelope of the incoming pulse with duration $\tau = 2T_0$, where T_0 is the period of the vibration at the central wavelength ($\lambda_0 = cT_0$). For example, $T_0 = 2.67$ fs and $\tau = 5.34$ fs at $\lambda_0 = 800$ nm. The amount of a primary aberration is determined by the parameter A_{lnm} in Eq. (16). The results of the calculation are shown in Fig. 3, 4 and 5. Pulse front predicted by the geometrical optics was also calculated from Eq. (62), and the results of the wave optical and the geometrical optical description were compared. The dashed curve shows the pulse front predicted by the geometrical optics.

Fig. 3 shows the spatial intensity distribution in the presence of primary spherical aberration characterized by $A_{040} = -6\,\lambda_0$ for moments $t = -7000\,T_0$, $-2394\,T_0$, $-1800\,T_0$ and $500\,T_0$ calculated from Eqs. (13), (31) and (32). The pulse front predicted by the geometrical optics calculated from Eqs. (62), (63) and (65) is illustrated by dashed curve. The geometrical caustic is shown by continuous line. The values of time t was chosen so that the pulse is in front of the focal region in case (a) and it is behind the focal region in case (d). In case (b) the pulse front propagating along the marginal rays just reaches the optical axis. Between the marginal and the paraxial focal point the pulse front has two parts. One of them is constructed along the paraxial rays so this part of the pulse front is (nearly) spherical. The other part of the pulse front is formed along the marginal rays. This is why this part has X shape spatial profile and the properties of this peak is very similar to the so-called Bessel-X wave pulses [39–41]. The X shaped part of the pulse front propagates with superluminal velocity along the optical axis and the radial intensity distribution resembles a Bessel-X wave pulse. Fig. 3a and 3d shows that in addition to the pulse front predicted by the geometrical optics an extra pulse appears. This pulse was termed *boundary wave pulse* in our previous publications [17, 19, 42, 43]. The appearance of boundary wave pulse is purely wave optical phenomenon, and it can be interpreted as the superposition of boundary diffraction waves [42–44]. Because of the aberration, the pulse front reaches the boundary of the exit pupil with a time delay $\Delta t = \Phi_a/c$, where $\Phi_a = \Phi_{040}(\rho = 1, \theta) = A_{040}$ is the aberration function at the edge of the exit pupil ($\rho = 1$). So the boundary diffraction waves are generated with a time delay $\Delta t = \Phi_a/c = A_{040}/c$ compared to the aberration-free case. Consequently the position z_b of the boundary wave pulse is shifted along the optical axis compared to the aberration-free case. The position of the boundary wave pulse is given by

$$\frac{z_b}{\lambda_0} = \frac{(t - \Delta t)/T_0}{1 - \frac{1}{2}\,(a/R)^2}. \tag{68}$$

The spatial intensity distribution in planes given by $\psi = 0°$ (meridional plane), $\psi = 45°$and $\psi = 90°$ (sagital plane) in the presence of primary coma characterized by $A_{031} = 2.5\,\lambda_0$ calculated from Eqs. (13), (37) and (38) at the time $t = -2000\,T_0$, $-200\,T_0$, 0, $200\,T_0$ and $2000\,T_0$ is depicted in Fig. 4. The pulse front predicted by the geometrical optics is illustrated by dashed curve. Cases (b), (c) and (d) show that in the vicinity of the paraxial image point the shape of the pulse front in the meridional plane forms a letter V. One can conclude that in the domain $y > 0$ there are points close to the paraxial image point and the meridional plane in which the pulse passes through twice.

The intensity distribution in the presence of primary astigmatism characterized by $A_{022} = 1.5\,\lambda_0$ is depicted in Fig. 5. The pulse front predicted by the geometrical optics is illustrated by dashed curve. In case (b) and (d) the pulse is situated at the sagital and meridional (tangential) focal line, respectively. In case (c) the pulse is at the circle of least confusion (in the middle between the sagital and the meridional focal lines).

In all of the three cases of the aberrations, in addition to the pulse front predicted by the geometrical optics, an extra pulse appears, which again can be interpreted as the superposition of boundary diffraction waves [42–44]

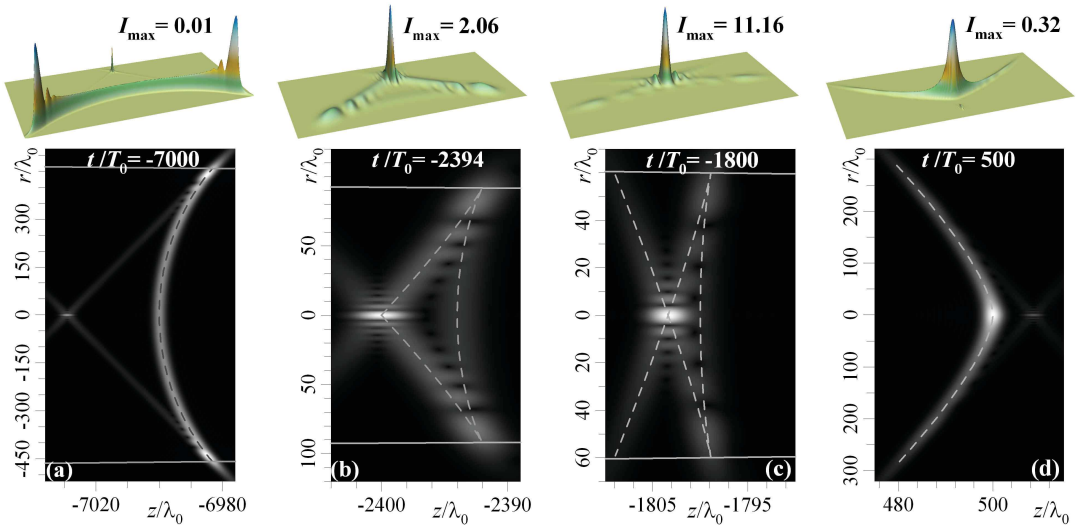

FIG. 3: Intensity distribution of a pulse with temporal duration $\tau = 2T_0$ at the time $t = -7000\,T_0$, $-2394\,T_0$, $-1800\,T_0$ and $500\,T_0$ in the presence of primary spherical aberration characterized by $A_{040} = -6\,\lambda_0$. The dashed curve shows the pulse front predicted by geometrical optics. The continuous lines indicates the geometrical caustic. The pulse is in front of the focal region in case (a) and it is behind the focal region in case (d). In case (b) the time was chosen so that the light pulse propagating along the marginal rays reaches the optical axis.

(see Figs. 3a, 3d, 4a, 4e, 5a and 5e). So the wave optical calculation shows that the boundary wave pulse appears not only in case of perfect imaging but in the presence of primary aberrations.

VI. CONCLUSIONS

In the present paper a theoretical, wave optical description of the effects of primary aberrations on the temporal and spatial shape of ultrashort pulses is presented. The calculations are based on the diffraction theory. The aberrations are expressed with the circular polynomials of Zernike, following the treatment by Nijboer and Zernike. The detailed formulas of the calculation, and the explicit form of the recurrence relations (30), (35) and (41) for the $A_j^{(p,q)}$ coefficients of the circular polynomial based expansion (26) are published, as far as we know, for the first time.

Numerical evaluation of the given expressions are depicted for primary spherical aberration (Fig. 3), primary coma (Fig. 4) and primary astigmatism (Fig. 5). Formalism for primary curvature of field and primary distortion are also given. The results for the spatio-temporal form of the pulse are compared with the pulse front shapes given by geometrical optical theory, also discussed in detail in the present paper. The pulse fronts show perfect correspondence between the geometrical and wave optical description.

The submitted figures also show that, in addition to the pulse front predicted by the geometrical optics, an extra pulse appears. This pulse is a pure wave optical phenomenon, called boundary wave pulse. This means that this superposition of boundary diffraction waves appears not only in case of aberration-free imaging, but also in the presence of primary aberrations.

Acknowledgments

The study was funded by the National Development Agency of Hungary under grant TECH-09-A2-2009-0134 and with financial support form the Research and Technology Innovation Fund (78549). The publication is supported by the European Union and co-funded by the European Social Fund. Project title: "Broadening the knowledge base and supporting the long term professional sustainability of the Research University Centre of Excellence at the University of Szeged by ensuring the rising generation of excellent scientists." Project number: TÁMOP-4.2.2/B-10/1-2010-0012.

[1] T. Brabec, F. Krausz. "Intense few-cycle laser fields: Frontiers of nonlinear optics", Rev. Mod. Phys. **72**, 545–591 (2000).
[2] G. A. Mourou, T. Tajima, S. V. Bulanov, "Optics in the relativistic regime", Rev. Mod. Phys. **78**, 309–371 (2006).
[3] S. Wang, Q. Gong, "Progress in femtochemistry and femtobiology", Sci. China Ser. A **54**, 2103–2108 (2011).
[4] S. E. Irvine, P. Dombi, G. Farkas, A. Y. Elezzabi, "Influ-

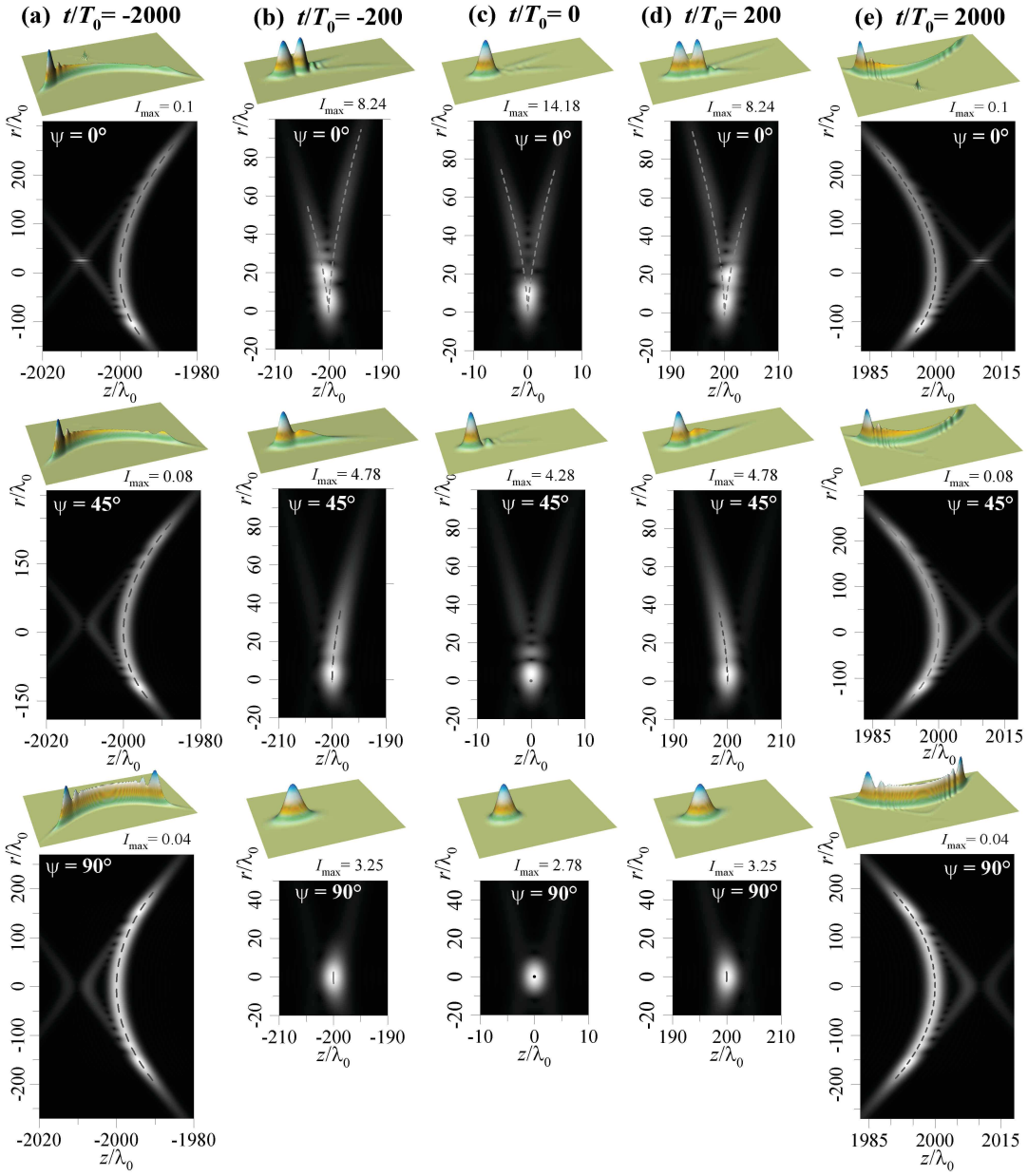

FIG. 4: Intensity distribution in planes given by $\psi = 0°$ (meridional plane), $\psi = 45°$and $\psi = 90°$ (sagital plane) for a pulse with temporal duration $\tau = 2T_0$ at the time $t = -2000\,T_0$, $-200\,T_0$, 0, $200\,T_0$ and $2000\,T_0$ in the presence of primary come characterized by $A_{031} = 2.5\,\lambda_0$. The dashed curve shows the pulse front predicted by geometrical optics. Cases (b), (c) and (d) show that in the vicinity of the paraxial image point the shape of the pulse front in the meridional plane forms a letter V. One can conclude that in the domain $y > 0$ there are points close to the paraxial image point and the meridional plane in which the pulse passes through twice.

ence of the carrier-envelope phase of few-cycle pulses on ponderomotive surface-plasmon electron acceleration", Phys. Rev. Lett. **97**, 146801 (2006).

[5] P. Dombi, S. E. Irvine, P. Rácz, M. Lenner, N. Kroó, G. Farkas, A. Mitrofanov, A. Baltuška, T. Fuji, F. Krausz, A. Y. Elezzabi, "Observation of few-cycle, strong-field phenomena in surface plasmon fields", Opt. Express **18**, 24206–24212 (2010).

[6] F. Krausz, M. Ivanov, "Attosecond physics", Rev. Mod. Phys., **81**, 163-234 (2009).

[7] C. Benedetti, P.Londrillo, T.V.Liseykina, A.Macchi, A.Sgattoni, G.Turchetti, "Ion acceleration by petawatt class laser pulses and pellet compression in a fast ignition scenario", Nucl. Instrum. Meth. A **606**, 89–93 (2009).

[8] Y. T. Alvin, H. Gibbs, JJ. Hu, A. M. Larson, "Advances in nonlinear optical microscopy for visualizing dynamic tissue properties in culture", Tissue Eng. Part B-Reviews **14**, 119–131 (2008).

[9] X. Peng, Y. Andegeko, D. Pestov, V. V. Lovozoy, M. Dantus, "Two-photon imaging using adaptive phase com-

pensated ultrashort laser pulses", J. Biomoed. Opt. **14**, 014002 (2009).
[10] P. S. Tsai, P. Blinder, B. J. Migliori, J. Neev, Y. S. Jin, J. A. Squier, D. Kleinfeld, "'Plasma-mediated ablation: an optical tool for submicrometer surgery on neuronal and vascular systems"', Curr. Opin. Biotech. **20**, 90–99 (2009).
[11] V. S. Yakovlev, P. Dombi, G. Tempea, C. Lemell, J. Burgdorfer, T. Udem, A. Apolonski, "Phase-stabilized 4-fs pulses at the full oscillator repetition rate for a photoemission experiment", Appl. Phys. B **76**, 329–332 (2003).
[12] B. Schenkel, J. Biegert, U. Keller, C. Vozzi, M. Nisoli, G. Sansone, S. Stagira, S. D. Silvestri, O. Svelto, "Generation of 3.8-fs pulses from adaptive compression of a cascaded hollow fiber supercontinuum", Opt. Lett. **28**, 1987-1989 (2003).
[13] A. L. Cavalieri, E. Goulielmakis, B. Horvath, W. Helml, M. Schultze, M. Fie, V. Pervak, L. Veisz, V. S. Yakovlev, M. Uiberacker, A. Apolonski, F. Krausz, R. Kienberger, "Intense 1.5-cycle near infrared laser waveforms and their use for the generation of ultra-broadband soft-x-ray harmonic continua", New J. Phys. **9**, 242 (2007).
[14] Zs. Bor, "Distortion of femtosecond laser-pulses in lenses and lens systems", J. Mod. Opt. **35**, 1907 (1988).
[15] Zs. Bor, "Distortion of femtosecond pulse in lenses", Opt. Lett. **14**, 119 (1989).
[16] Zs. Bor, "Femtosecond-resolution pulse-front distortion measurement by time-of-flight interferometry", Opt. Lett. **14**, 862 (1989).
[17] Zs. Bor and Z. L. Horvath, "Distortion of femtosecond pulse in lenses. Wave optical description", Opt. Commun. **94**, 249 (1992).
[18] Z. L. Horvath and Zs. Bor, "Focusing of femtosecond pulses having Gaussian spatial distribution", Opt. Commun. **100**, 6 (1993).
[19] Z. L. Horvath and Zs. Bor, "Behaviour of femtosecond pulses on the optical axis of a lens. Analytical description", Opt. Commun. **108**, 333 (1994).
[20] Zs. Bor and Z. L. Horvath, "How to select a lens for focusing of femtosecond pulses", Braz. J. Phys. **26**, 516 (1996).
[21] A. Federico, O. Martinez, "Distortion of femtosecond pulses due to chromatic aberration in lenses", Opt. Commun. **91**, 104 (1992).
[22] M. Kempe, U. Stamm, B. Wilhelmi and W. Rudolph, "Spatial and temporal transformation of femtosecond laser-pulses by lenses and lens systems", J. Opt. Soc. Am. B **9**, 1158 (1992).
[23] D. Zalvidea, "Phase mask for spatial and temporal control of ultrashort light pulses focused by lenses", J. Opt. Soc. Am. A **20**, 1981 (2003).
[24] W. Amir, T. A. Planchon, C. G. Durfee, J. A. Squier, P. Gabolde, R. Trebino, M. Müller, "Simultaneous visualization of spatial and chromatic aberrations by two-dimensional Fourier transform spectral interferometry", Opt. Lett. **19**, 2927–2929 (2006).
[25] H.-M. Heuck, P. Neumayer, T. Kuehl, U. Wittrock, "Chromatic aberration in petawatt-class lasers", Appl. Phys. B **84**, 421–428 (2006).
[26] M. Kempe and W. Rudolph, "Impact of chromatic and spherical-aberration on the focusing of ultrashort light-pulses by lenses", Opt. Lett. **18**, 137 (1993).
[27] M. Kempe and W. Rudolph, "Femtosecond pulses in the focal region of lenses", Phys. Rev. A **48**, 4721 (1993).
[28] D. Zalvidea and E. E Sicre "Ultrashort light pulse propagation in aberrant optical systems: spatialtemporal analysis", J. Opt. A: Pure Appl. Opt. **5** S310 (2003)
[29] G. O. Mattei, M. A. Gil, "Spherical aberration in spatial and temporal transforming lenses of femtosecond laser pulses", Appl. Opt. **38**, 1058–1064 (1999).
[30] M. A. Gonzalez-Galicia, M. Rosete-Aguilar, J. Garduno-Mejia, N. C. Bruce, R. Ortega-Martinez, "Effects of primary spherical aberration, coma, astigmatism and field curvature on the focusing of ultrashort pulses: homogenous illumination", J. Opt. Soc. Am. A **28**, 1979–1989 (2011).
[31] M. A. Gonzalez-Galicia, J. Garduno-Mejia, M. Rosete-Aguilar, N. C. Bruce, R. Ortega-Martinez, "Effects of primary spherical aberration, coma, astigmatism, and field curvature on the focusing of ultrashort pulses: Gaussian illumination and experiment", J. Opt. Soc. Am. A **28**, 1990–1994 (2011).
[32] P. Bowlan, P. Gabolde, R. Trebino, "Directly measuring the spatio-temporal electric field of focusing ultrashort pulses", Opt. Express **16**, 10219–10230 (2007).
[33] P. Bowlan, U. Fuchs, R. Trebino, U. D. Zeitner, "Measuring the spatiotemporal electric field of tightly focused ultrashort pulses with sub-micron spatial resolution", Opt. Express **18**, 13663–13675 (2008).
[34] K. Mecseki, A. P. Kovács, Z. L. Horváth, "Measurement of Pulse Front Distortion Caused by Aberrations Using Spectral Interferometry.", AIP Conf. Proc. **1228**, 190–196 (2010).
[35] C. Bourassin-Bouchet, S. de Rossi, F. Delmotte, P. Chavel, "Spatiotemporal distortions of attosecond pulses", J. Opt. Soc. Am. A **27**, 1395–1403 (2010).
[36] M. Born and E. Wolf, *Principles of Optics*, (Pergamon Press, Oxford, 1987), chap. IX.
[37] Z. L. Horvath, A. P. Kovacs, Zs. Bor, "Distortion of ultrashort pulses caused by aberrations", Springer Ser. Chem. Phys. **88**, 220–222 (2007).
[38] A. Prata, W. V. T. Rusch, "Algorithm for computation of Zernike polynomials expansion coefficients", Appl. Opt. **28**, 749–754 (1989).
[39] J. Lu and J. F. Greenleaf, "Nondiffracting X waves-exact solutions to free-space scalar wave equation and their finite aperture realizations.", IEEE Trans. Ultrason. Ferroelec. Freq. Contr. **39**, 19 (1992).
[40] J. Fagerholm, A. T. Friberg, J. Huttunen, "Angular-spectrum representation of nondiffracting X waves", D. P. Morgan and M. M. Salomaa, Phys. Rev. E **54**, 4347 (1996).
[41] P. Saari and K. Reivelt, "Evidence of X-Shaped Propagation-Invariant Localized Light Waves", Phys. Rev. Lett. **79**, 4135 (1997).
[42] Z. L. Horvath and Zs. Bor, "Diffraction of short pulses with boundary diffraction wave theory", Phys. Rev. E **63**, 26601 (2001).
[43] Z. L. Horvath, J. Klebniczki, G. Kurdi, A. P. Kovács, "Experimental investigation of boundary wave pulse", Opt. Commun. **239**, 243 (2004).
[44] P. Saari, P. Bowlan, H. Valtna-Lukner, M. Lõhmus, P. Piksarv, R. Trebino, "Basic diffraction phenomena in time domain", Opt. Express **18**, 11083–11088 (2010).

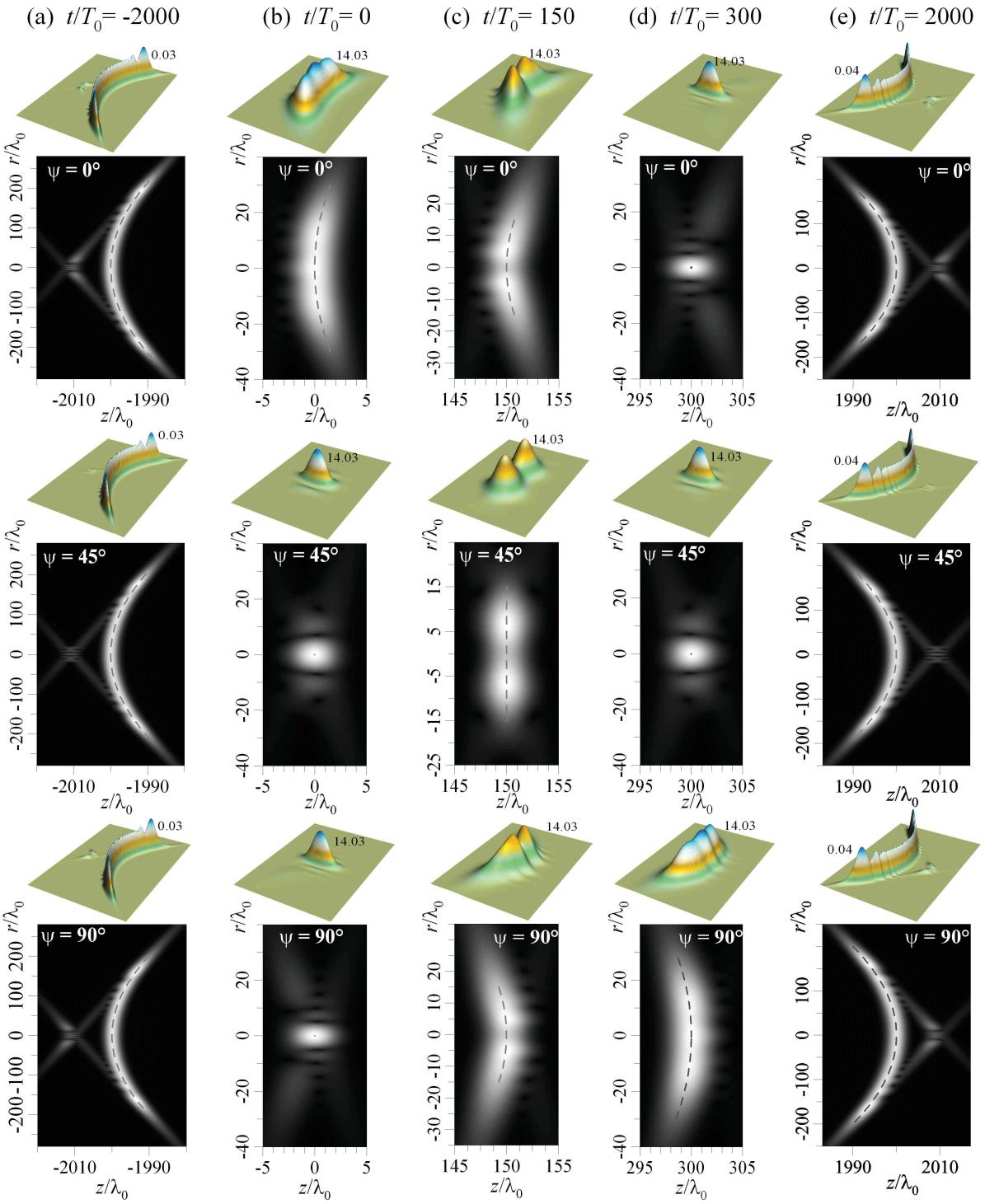

FIG. 5: Intensity distribution in planes given by $\psi = 0°$ (meridional plane), $\psi = 45°$and $\psi = 90°$ (sagital plane) for a pulse with temporal duration $\tau = 2T_0$ at the time $t = -2000\,T_0$, 0, $150\,T_0$, $300\,T_0$ and $2000\,T_0$ in the presence of primary astigmatism characterized by $A_{022} = 1.5\,\lambda_0$. The dashed curve shows the pulse front predicted by the geometrical optics. In case (b) and (d) the pulse is situated at the sagital and meridional (tangential) focal line, respectively. In case (c) the pulse is at the circle of least confusion (in the middle between the sagital and the meridional focal lines).